



ISSN: 2230-9926

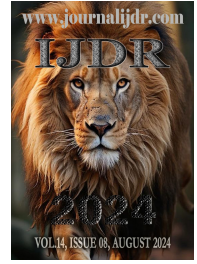
Available online at <http://www.journalijdr.com>

IJDR

International Journal of Development Research

Vol. 14, Issue, 08, pp. 66496-66505, August, 2024

<https://doi.org/10.37118/ijdr.28650.08.2024>



RESEARCH ARTICLE

OPEN ACCESS

CHARACTERIZATION OF NATURAL STONES USED FOR THE CONSTRUCTION OF THE FORT IKOMA HISTORICAL BUILDING IN SERENGETI NATIONAL PARK, TANZANIA

*^{1,2}Rajab Ayubu Chuo, ¹Patrice Nyangi and ¹Gislar Kifanyi

¹Department of Civil Engineering, College of Engineering and Technology, Mbeya University of Science and Technology, P.O. Box 131, Mbeya, Tanzania

²Department of Infrastructure, Tanzania National Parks, P. O. Box 3134, Arusha, Tanzania

ARTICLE INFO

Article History:

Received 27th May, 2024
Received in revised form
18th June, 2024
Accepted 06th July, 2024
Published online 30th August, 2024

Key Words:

Fort Ikoma; Natural Stones; Physical Analysis; Porosity; Serengeti National Park.

Corresponding Author: Rajab Ayubu Chuo

ABSTRACT

The conservation and restoration of heritage buildings, mostly Fort Ikoma in Serengeti National Park (SENAPA), Tanzania, requires a thorough understanding of the materials originally used. This study aimed to investigate the physical, chemical, mineralogical, and petrographic properties of the natural stones used in Fort Ikoma's construction using standard methods. The analysis revealed that the fort was constructed using two types of natural stones: reddish-brown shale and light-grey limestone. The shale, recommended for building, consists mainly of quartz (30%), dickite (19%), illite (12%), sepiolite (7.4%), calcite (6%), and nepheline (5.4%). The limestone, accepted as a building stone, was of very high purity, composed primarily of calcite (64.3%), with quartz (8.7%), vaterite (6.5%), and dolomite (5%) as significant constituents. For the restoration of Fort Ikoma, it is recommended to use limestone for the foundation and lower walls and shale for the superstructure. These findings enhance understanding of historical materials and support the restoration of Fort Ikoma and similar structures.

Copyright©2024, Rajab Ayubu Chuo et al. This is an open access article distributed under the Creative Commons Attribution License, which permits unrestricted use, distribution, and reproduction in any medium, provided the original work is properly cited.

Citation: Rajab Ayubu Chuo, Patrice Nyangi and Gislar Kifanyi. 2024. "Characterization of natural stones used for the Construction of the fort Ikoma Historical Building in Serengeti National Park, Tanzania". International Journal of Development Research, 14, (08), 66496-66505.

INTRODUCTION

Masonry is one of the primitive building materials that have been used all over the world for construction since the beginning of the earliest civilizations due to the simplicity of building techniques and the features that characterize these materials (Amer *et al.*, 2020). Earliest construction embraces immense worth in cultural, historical, and archeological importance, standing as a testament to the originality of past civilizations and craftsmanship at the global level. These classical milestones imbued with cultural heritage, historical legacy, and architectural marvels yield tangible links to the collective identity of historical epochs. The ancient constructional artifacts are considered precious assets that contribute to tourism and foster a deep understanding of construction methodologies practiced throughout antiquity (B. S. Ali *et al.*, 2024). Natural stones, such as building stones, have been broadly used by humans since the dawn of time ages. It mainly comprises limestone, slate, shale, sandstone, marble, and so on. The colors and textures of the natural stones depend on the rock. The building stones used for construction must meet the high-quality standards of engineering properties to secure the building against all conditions (Bukhari *et al.*, 2023). Historical or heritagestone-built buildings, cultural heritage artifacts, and monuments are vulnerable due to hazards of all kinds from anthropic to natural (Pereira, 2024).

The main causes of the deterioration of natural stone materials exposed to external conditions and employed as either construction material or decoration are time and atmospheric agents (rain, wind, solar radiation, aggressive atmospheric pollutants, freeze-thaw cycles, crystallization of saline solutions, and growth of organisms) (Pappalardo *et al.*, 2022). Natural stones have been used for many years in many historically and culturally important structures. (Pereira and Marker, 2016). Natural stones decayed over time at higher rates when placed outside of their natural environment. They undergo deterioration processes when exposed to weathering, thus because of their intrinsic properties (porosity, permeability, mineralogy), extrinsic properties (fluid circulation, environment, climatic condition), and anthropogenic factors. The anthropic hazards can be stopped or prevented before it is too late to face fatal consequences and natural hazards are inevitable (Pereira, 2024) and (Hernández *et al.*, 2024). This deterioration can lead to loss of value, loss of physical properties, and lastly can lead to ruins of historical buildings. Strategies to prevent or protect the stone-built heritage include that if the replacement of stone is necessary, a major effort should be made to identify the stone that was used originally, ensuring that the replacement does not affect either the aesthetics or the cultural value. This approach is a reality in places where the natural conditions are destroying valuable heritage and the identification of the stone remains vague (Pereira, 2023).

Therefore, studying the characteristics of natural stones to understand their ingenuity can help in conservation and restoration work (Hernández *et al.*, 2024). Stones similar or closely similar to the original natural stones should be used during conservation and restoration work. The use of incompatible stones can be aesthetically insightfully or have structurally and financially damaging consequences (Pereira and Marker, 2016). Historical buildings pose numerous challenges for diagnosis and restoration because of limited construction records, diverse and variable materials, restricted access, and limitations on sample extraction, which hinder the use of modern technical standards and building codes (Cintra *et al.*, 2024). The historical significance of Fort Ikoma, firstly constructed as a stone masonry fort by Germans and later utilized by British colonial and Tanzanian post-independence governments, underscores the need for its preservation. Historical stone masonry structures like Fort Ikoma often face risks such as material fatigue, environmental loads, and inadequate original construction techniques (Lourenço, 2002). The historical fabric of such buildings reflects the knowledge and experience of past builders, often devoid of modern scientific and engineering standards (Mustafaraj, 2013). Fort Ikoma, located in SENAPA, Tanzania, serves not only as an architectural and historical landmark but also as a significant asset with potential economic benefits through tourism. However, the fort has deteriorated significantly due to prolonged neglect and structural weaknesses, necessitating a comprehensive assessment and restoration plan.

Coupled Plasma Atomic Emission Spectrometer (Perkin-Elmer Elan 6000 or 9000) following Lithium metaborate/tetraborate fusion and dilute nitric digestion to determine the major oxides and rare earth elements were analyzed by ICP Mass Spectrometry and loss on ignition (LOI) was determined by measuring the weight loss after heating (Okunlola *et al.*, 2023).

The deterioration process of limestone in the Anahita Temple of Kangavar (West Iran), its chemical and mineralogical analysis of stones, characterization of deterioration patterns and processes, and identification of factors influenced the process obtained by on-site and laboratory studies, including optical microscopy, petrography, X-ray fluorescence, X-ray diffraction and scanning electron microscopy coupled with energy dispersive X-ray spectroscopy methods (Barnooset *et al.*, 2020). Unfortunately, there is limited information concerning the characterization of natural stones used in the Fort Ikoma historical building in SENAPA, Tanzania through physical, chemical, mineralogical, and petrographic analysis. This research employed modern analytical techniques such as X-ray fluorescence (EDXRF), X-ray diffraction (XRD), and reflected and transmitted light microscopy to characterize the natural stones. The findings from this investigation will contribute to the growing body of knowledge on historical construction materials and to develop restoration strategies for historical buildings like the Fort Ikoma historical building in Serengeti National Park, Tanzania (Degryse *et al.*, 2002).

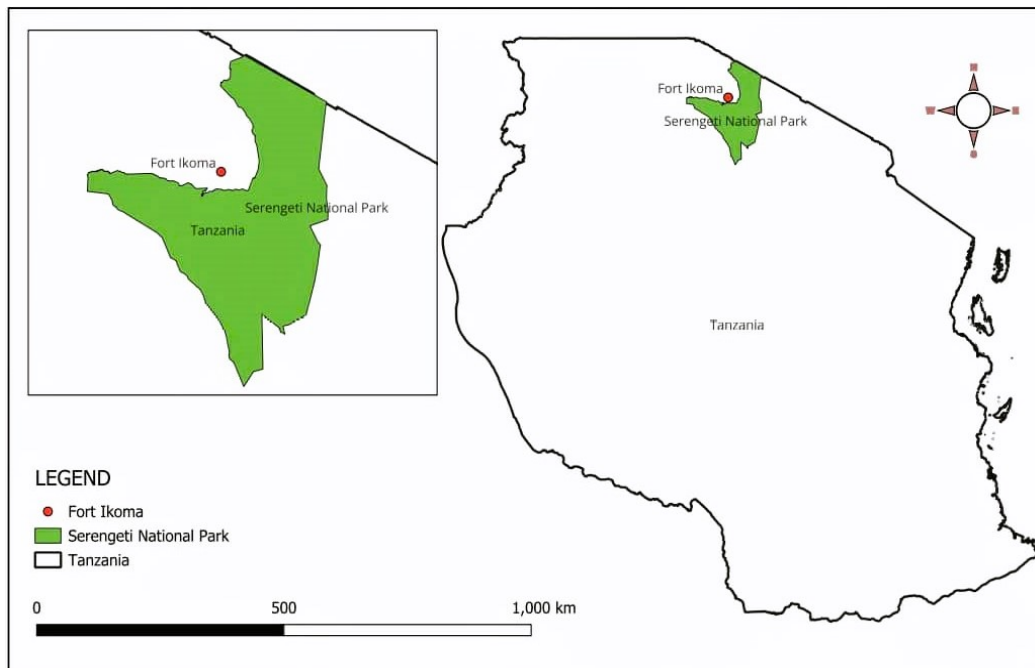


Figure 1. Map showing the location of Fort Ikoma historical building in SENAPA

The preservation and restoration of historical buildings hold paramount importance for maintaining cultural heritage and ensuring its transmission to future generations (Lucian, 2008). The primary purpose of this study is to assess and develop restoration strategies for the Fort Ikoma Historical Building in SENAPA, Tanzania, focusing on the physical, chemical, mineralogical, and petrographic properties of the natural building stones used in its construction. Understanding the characteristics of the natural building stones and their possible damage and proposing their possible solutions is crucial for developing sustainable conservation and restoration strategies that respect the building's architectural, historical, and cultural significance while ensuring its longevity (Hernández *et al.*, 2024). Mineralogical analysis of shales within the Lower Anambra Basin, Nigeria was conducted by using an X-ray Diffractometer with the aid of a Radicon MD 10 Diffractometer. The diffractogram interpretation was done by comparing the peaks to standard minerals established by the International Center for Diffraction Data (ICDD), in 2008 and 2009. Geochemical analysis was conducted by using an Inductive

MATERIALS AND METHODS

Description of the Study Area: Geographically, Fort Ikoma is located in the Ikoma ward of the Serengeti district in the Mara region (36M 0682369 UTM 9769712, Map Datum Arc 1960) as shown in (Figure.1). It is one of many Forts built across Tanzania during the German colonial rule from 1885 to 1918. Unlike other German forts built in urban areas, the Fort Ikoma is situated in an area abundant with wildlife. Administratively, Tanzania National Parks (TANAPA) through SENAPA is the owner and overseer of the Fort.

Visual Inspections: The study of stone masonry walls has various aims concerning diagnosis and restoration work. The conducted field survey by visual inspection focused on the construction technology of stone masonry walls, building materials, the overall wall thickness, the composition of the inner core layer, and the connectivity between the walls' leaves (Amer *et al.*, 2021).

Sampling: Through visual investigations, two different types of stone materials were identified (sample 1B and sample 2A) (Figure.2), these samples were collected from areas without aesthetic value or from severely damaged parts. The samples (25numbers) were derived from the outer and inner layers, the ratio between inner and external leaves, the bed and head joints of the outer layer, and the inner core layer (Amer *et al.*, 2021).

properties of the natural stone, as outlined in ASTM C-97-09 (010) (Surdashy and Aqrawi, 2023). The apparent density is calculated using the following equation (1) (CML, 2000).

$$\rho = \left(\frac{A}{(A - M_{sat}) / 0.997} \right) \dots\dots\dots(1)$$

Where: ρ is the apparent density (g/cm^3), A is the dry weight of the sample, and M_{sat} is the mass of saturated sample in water.



Figure 2. Identified two different natural stone samples used for the construction of the Fort Ikoma historical building in SENAPA, Tanzania

Sample Condition and Nature: The samples are grey to reddish brown (1B) and light grey (2A) colored and composed of clay materials, angular to sub-angular silt to sand-sized grains of quartz and feldspars. The samples have a granular texture, their constituent grains were very fine. These samples were weathered and altered in this case a prolonged weathering and alteration of the silicate-bearing rocks led to the formation of clay-related minerals. The reddish-brown color of the shale sample is due to the presence of iron oxide and hydroxide-related minerals.

Moisture Content (M.C): Water presence in natural stone can alter its properties and behavior, especially if clay is present, as it softens the material, loosens its structure, and increases deformability, ultimately reducing the stone's overall strength. Water can lower the shear resistance of joint sets, depending on pore water pressure. Rock strength decreases as moisture content rises, making water content a crucial factor influencing natural stone strength (Hagan, 2009). The basic properties of the natural stone influence the durability and elasticity of the natural stone through freezing and thawing processes, moisture content depends on the porosity, density, and permeability of the natural stone and is measured by the weight of the water in the natural stone volume (W_w) to the dry weight of the natural stone volume (W_d) according to ASTM C-127-01 (004), shown in equation (2)(Surdashy and Aqrawi, 2023).

$$M. C = \left(\frac{W_w}{W_d} \right) * 100 \dots\dots\dots(2)$$

Where: M.C.= moisture content

Physical Characteristics Analysis: The physical characteristics of the stones including apparent density, moisture content, apparent specific gravity, porosity, and water absorption were determined according to (CML, 2000), (Surdashy and Aqrawi, 2023) and (the Bureau of Indian Standards, 2003). The stones sample used were those crushed into pieces and then passed through the 20mm IS sieve. The sample about 1 kg in weight, is washed to make clean and immersed in the jar of water at room temperature for 24 hours. After 24 hours, the sample is taken out and spread on a cloth to dry its surface, but away from direct sunlight or any heat source, for not less than 10 min. The weight of the sample is then measured (B). The sample is again kept in a vessel and water is poured into it until it shows a 1000 ml mark. The quantity of water added is then recorded (C). The sample is then taken out of the vessel and dried in an oven at $100^{\circ}C$ for a minimum of 24 hours. The weight of the sample is measured after cooling (A) (Patil *et al.*, 2021). Equations (1), (2), (3), (4), and (5) measured the physical characteristics of the natural stone from the Fort Ikoma historical building.

Apparent Specific Gravity (A.S.G): The apparent specific gravity of natural stone is the ratio of the mass of a given volume of the natural stone to the mass of a volume of water equal to the volume of the solid matter and impermeable voids of the natural stone (Mifkovicet *et al.*, 2012). Expressed as a numerical value for the saturated surface-dry sample at the recorded temperature, shown in equation (3)(Bureau of Indian Standards, 2003).

$$\text{Apparent specific gravity} = \frac{A}{1000 - \dots} \dots\dots\dots(3)$$

Water Absorption (W.A): The water absorption of the natural stone is the amount of water absorbed by a natural stone. It is calculated as the ratio of the weight of water absorbed to the weight of the dry material. Expressed as the percentage by weight of the oven-dry sample, shown in equation (4) (Bureau of Indian Standards, 2003).

$$\text{Water absorption} = \left(\frac{B - A}{A} \right) * 100 \dots\dots\dots(4)$$

Apparent Density (ρ): Natural stone density is a substantial property and varies in different stones depending on the mineralogy and compaction of a rock. It is usually measured in g/cm^3 (B. Ali *et al.*, 2023). A natural stone sample's apparent density is defined as the dry sample's mass per unit volume. Compared to wet density values, apparent density tends to vary within narrower limits because the mineral composition and porosity of the natural stone influence it. Natural stones with low porosity and a high proportion of solid components generally exhibit higher dry densities. Moreover, the apparent density of natural stones/rocks increases with depth. Both density and porosity are crucial factors that influence the mechanical

Apparent Porosity (A.P): Apparent porosity of natural stone means the ratio of open pores in the natural stone to its total volume of the

natural stone. Apparent porosity analysis is the non-destructive analysis of the building stones. The porosity is measured with the following equation (5) (Patil *et al.*, 2021);

$$\text{Apparent porosity} = \left(\frac{B-A}{1000-A} \right) * 100 \quad (5)$$

Chemical Characteristics Analysis: Chemical characteristics analyses were performed using a Rigaku NEX CG most advanced energy dispersive XRF (EDXRF) spectrometer and it is a non-destructive analysis. The Rigaku NEX CG is an Energy Dispersive X-ray Fluorescence (EDXRF) spectrometer for elemental analysis of Sodium (Na) to Uranium (U) in solid, liquid, and powder samples as well as thin film coatings on solid substrates. In EDXRF low energy “soft” X-rays (1-50keV) are emitted from an X-ray tube. These source X-rays enter the sample and cause the atoms in the sample to fluoresce their characteristic low-energy “soft” X-rays. These fluorescent X-rays are captured in a detector and counted by a multi-channel analyzer. The NEX CG software then calculates the concentration of each element present in the sample from Sodium to Uranium. A powerful and easy-to-use QuantEZ® software interprets XRF with a multilingual user interface.

Calibration of Rigaku NEX CG EDXRF spectrometer: The spectrometer machine was first calibrated using a Multi-Channel Analyzer (MCA) calibration sample to calibrate the relationship between the channels of spectrum data and energy of fluorescent X-rays and the standard results Fe=663keV, Ba= 470keV, and K= 356keV were obtained. Then the library calibration was conducted. In the library calibration, the peak profiles of elements are obtained using Sn, Cu, and SiO₂ samples, and the peak profiles are calibrated. The fluorescent X-ray intensities of elements contained in the MCA sample are also obtained to carry out the drift calibration of sensitivity library measurement intensities. If this calibration is not carried out for a long period, library data will not correlate with the data of samples because of variations in peak profiles and X-ray intensities, and erroneous identifications and shifts of analysis value will result. Afterward, sample pellets were loaded and analyzed on the EDXRF spectrometer. The obtained sample results were evaluated using NEX CG software, normalized, and finally printed for reporting.

Limestone Purity Classification: According to Harrison, (1993) and Teodorovich, (1950) classification, the CaCO₃% carried out by the Folks equation (6) (Surdashy and Aqrawi, 2023).

$$\text{CaCO}_3 = \left(\frac{\text{CaCO}_3 \text{ molecular weight}}{\text{CaO molecular weight}} \right) * \text{CaO}\% \quad (6)$$

Mineralogical Characteristics Analysis: XRD analysis is the rapid analytical technique mainly used for the phase identification of crystalline minerals and provides information on the sample's unit cell dimensions and chemical composition. In XRD analysis, the X-ray is permitted to pass through each element of the sample, and then deflected, identification of the elements from the sample is done by this deflection (Patil *et al.*, 2021). Mineralogical characteristics analyses were conducted at ambient temperature using a Rigaku MiniFlex benchtop X-ray diffractometer. The applied equipment conditions were Cu-K α radiation, $\lambda = 1.5405 \text{ \AA}$, from 3° to 70° (2 θ) explored range, 0.11° 2 θ /s scanning rate. Its XRD patterns were interpreted using the latest SmartLab Studio – II software, Rigaku's full-function powder diffraction analysis package. The software provides various analysis tools such as automatic phase identification, quantitative analysis, crystallite-size analysis, lattice constants refinement, Rietveld analysis, and ab initio structure determination. The rock samples were first crushed and dried at a temperature of 70 degrees centigrade to reduce moisture content, homogenized then split into two parts. One half was stored for future reference and the second half was pulverized to get a fine powder of approximately 75 microns.

Petrographic Characteristics Analysis: Petrographic characteristics analyses were executed using Leica reflected and transmitted light

microscopy. A petrographic or thin section was used to analyze the natural stones from the Fort Ikoma historical building. The thin sections were analyzed using a Leica DM 750P polarizing light microscope.

Thin Section Sample Preparations: The rock chips of 4-5mm were cut by a diamond-impregnated cutting saw from big to small size rock samples (rock chips), then the rock chips were clearly labeled, dried, and mounted onto glass slides so that two different standard petrographic thin sections were prepared from each sample by using standard procedure for preparing thin section. The standard (30 microns) thin sections were made ready for petrographic analysis.

Illustration Images: The images were taken with a Leica camera at X50 magnification, several images were taken at x100 magnification depending on the features observed. The images were taken at the 1600 x 1200 pixels size at a calibration of 1 pixel = 1 pixel. The field of view for all samples is 7mm.

RESULTS AND DISCUSSION

These results were evaluated through EDXRF, X-ray diffraction (XRD), and reflected and transmitted light microscopy tests.

Visual investigations: Most of the masonry walls were single-leaf and multi-leaves and consisted of three leaves. Two outer leaves (superstructure walling) were well-dressed stones of sample 1B and jointed by mud mortar, the outer leaves stones were either pointed by cement/sand materials or fully plastered by cement/sand materials of about 0.03 to 0.05m to protect the wall against weathering effect. The inner core was filled by different samples (1B and 2A) but mostly 1B. The average wall thicknesses from end to end of the outer leaves were about 0.8 to 1.2m, with a thickness ratio between external and internal leaves of about 0.10 to 0.25m. The walls were much thicker at the foundation and floor levels, and wall thickness started to reduce as the height of the superstructure increased. Sample 2A was mostly used on foundation and floor level walling (Figure 4) and sample 1B was mostly used on superstructure walling (Figure 3) also in floor slab, and foundation walling. Some of the stone walls were observed weathered and some walls collapsed due to long exposure to weather (Figure 5).



Figure 3. Sample 1B was used for superstructure walling



Figure 4. The picture shows the foundation wall that was built by sample 2A



Figure 5. The picture showed a collapsed stone masonry wall

Physical characteristics: The results of the physical properties of samples 1B and 2A were obtained from the laboratory as shown in (Table 1) and (Table 2).

The durability of the samples depends on water absorption and apparent porosity, the higher the values the more porous the samples. The minimum moisture content showed that sample 1B was dry

Table 1. Physical properties value of natural stones sample 1B

Specimen Reference		1	2	3	Mean
Mass of oven-dry aggregate in the air (A)	g	987.10	984.00	985.00	985.37
Mass of saturated surface dry sample + pycnometer	g	1794.00	1792.00	1792.70	1792.90
Mass of saturated surface dry aggregate in air (B)	g	1026.00	1024.00	1024.00	1024.67
Mass of saturated sample + pycnometer + water	g	2388.00	2368.00	2388.00	2381.33
Quantity of water added (C)	g	594.00	576.00	596.00	588.67
Volume of pycnometer	g	1000.00	1000.00	1000.00	1000
Mass of clean dry pycnometer	g	768.00	768.00	768.00	768
Apparent Specific Gravity (A.S.G)	g/cm ³	2.43	2.32	2.44	2.40
Apparent Density (ρ)	g/cm ³	2.70	2.58	2.71	2.66
Water Absorption (W.A)	%	3.94	4.07	3.96	3.99
Apparent Porosity (A.P)	%	9.58	9.43	9.65	9.55
Moisture Content Determination					
Tin Number		E11	E26	E58	Mean
Tin+Wet sample (G)	g	391.10	380.30	398.10	389.83
Tin+Dry sample (F)	g	389.10	378.60	396.00	387.90
Weight of the water in the sample (G-F) or Ww	g	2.0	1.7	2.1	1.93
Weight of Dry sample (F-T) or Wd	g	302.1	292.4	312.1	302.20
Tin alone (T)	g	87.00	86.20	86.00	86.33
Moisture Content (M.C)	%	0.66	0.58	0.67	0.64

Table 2. Physical properties value of natural stones sample 2A

Specimen Reference		1	2	3	Mean
Mass of oven-dry aggregate in the air (A)	g	984.70	985.30	988.00	986.00
Mass of saturated surface dry sample + pycnometer	g	1847.00	1845.90	1849.70	1847.53
Mass of saturated surface dry aggregate in air (B)	g	1071.00	1069.90	1073.70	1071.53
Mass of saturated sample + pycnometer + water	g	2380.00	2380.00	2380.00	2380
Quantity of water added (C)	g	533.00	534.10	530.30	532.47
Volume of pycnometer	g	1000.00	1000.00	1000.00	1000
Mass of clean dry pycnometer	g	776.00	776.00	776.00	776
Apparent Specific Gravity (A.S.G)	g/cm ³	2.11	2.12	2.10	2.11
Apparent Density (ρ)	g/cm ³	2.60	2.60	2.59	2.59
Water Absorption (W.A)	%	8.76	8.59	8.67	8.67
Apparent Porosity (A.P)	%	18.48	18.16	18.25	18.30
Moisture Content Determination					
Tin Number		F20	F40	F36	Mean
Tin+Wet sample (G)	g	490.10	381.30	493.70	455.03
Tin+Dry sample (F)	g	486.40	378.60	490.10	451.70
Weight of the water in the sample (G-F) or Ww	g	3.7	2.7	3.6	3.33
Weight of Dry sample (F-T) or Wd	g	399.4	292.4	404.1	365.30
Tin alone (T)	g	87.00	86.20	86.00	86.33
Moisture Content (M.C)	%	0.93	0.92	0.89	0.91

Table 3. Density classification according to ASTM C-97-09, and porosity classification of building stone according to Levorson, (1970), Surdasy and Aqravi, (2023)

ASTM C-97-09 (010) Classification		Levorson, 1970 Classification	
Density gm/cm ³	Classification	Porosity %	Classification
< 1.8	Very low	<5	Not present
1.8-2.2	Low	5-10	Low
2.2-2.55	Medium	10-15	Medium
2.55-2.75	High	15-25	High
>2.75	Very high	>25	Very high

Sample 1B: Suitability for building stone in terms of density and porosity according to ASTM C-97-09 (010) and Levorson, 1970 Classification, revealed that sample 1B ($\rho=2.66\text{g/cm}^3$ and A.P= 9.55%) was of high density and low porosity, which was recommended as a building stone (Surdasy and Aqravi, 2023).

Sample 2A: In terms of density and porosity according to ASTM C-97-09 (010) and Levorson, (1970 Classification) of building stone, revealed that sample 2A ($\rho=2.59\text{g/cm}^3$ and A.P= 18.30%) was of high density and high porosity, which was accepted as a building stone (Surdasy and Aqravi, 2023). All samples revealed that the moisture contents increased as the water absorptions increased as the increased of porosity of the natural stones, the higher value indicated that the materials were highly porous.

compared to sample 2A with more moisture content. The apparent density increased as apparent specific gravity increased, the higher the amount the more the natural stone is suitable for construction. Suitability of limestone rocks in Erbil, Kurdistan Region of Iraq for building stone in terms of dry density and porosity according to ASTM C-97-09 (010) and Levorson, 1970 Classification showed that KF ($\rho=2.02\text{g/cm}^3$ and A.P= 15.64%) and QSA ($\rho=2.08\text{g/cm}^3$ and A.P= 17.61%) were of low density and high porosity, which were accepted as building stone. Moreover, PtS ($\rho=2.44\text{g/cm}^3$ and A.P=8.63%), SS ($\rho=2.33\text{g/cm}^3$ and A.P= 10.50%), HS ($\rho=2.39\text{g/cm}^3$ and A.P= 9.00%), and ShS ($\rho=2.22\text{g/cm}^3$ and A.P= 12.14%) were of medium density and porosity, which were highly recommended as building stone, and BQ ($\rho=2.84\text{g/cm}^3$ and A.P= 2.90%), SA ($\rho=2.68\text{g/cm}^3$ and A.P= 5.20%), PmP ($\rho=2.02\text{g/cm}^3$ and A.P= 15.64%),

BK($\rho=2.02\text{g/cm}^3$ and A.P= 15.64%), and QNE($\rho=2.64\text{g/cm}^3$ and A.P= 6.13%) were of high to very high density and low to no porosity in them, which were recommended as building stone, shown in (Table. 3) (Surdashy and Aqrawi, 2023). Besides, showed that the apparent specific gravity is directly proportional to its dry density and the amount of water content is directly proportional to its water absorption, and porosity (Surdashy and Aqrawi, 2023).

Chemical characteristics: The chemical composition analysis results for two stone samples, 1B and 2A, from the Fort Ikoma historical building. The results were provided as percentages for various oxide compounds shown in (Table. 4).

Table 4. Chemical compositions for samples 1B and 2A (% by weight)

S/N	Chemical composition	Sample 1B	Sample 2A
1.	SiO ₂ %	63.27	7.49
2.	Al ₂ O ₃ %	18.61	2.44
3.	Na ₂ O %	1	<0.01
4.	K ₂ O %	3.60	0.30
5.	Fe ₂ O ₃ %	11.72	1.17
6.	MgO %	0.39	0.72
7.	CaO %	0.10	87.37
8.	SO ₂ %	<0.01	0.18
9.	TiO ₂ %	1.19	0.15
10.	P ₂ O ₅ %	<0.01	0.17
11.	BaO %	0.12	<0.01
12.	MnO %	<0.01	<0.01
13.	SrO %	<0.01	<0.01
14.	Cl %	<0.01	<0.01

NB:<0.01% means the parameter reading is less than the lowest detection limit which is 0.01%

Sample 1B: The main chemical constituent of sample 1B was silica (SiO₂) at 63.27%, and other constituents were alumina (Al₂O₃) at 18.61%, iron (III) oxide (Fe₂O₃) at 11.72%, potassium oxide (K₂O) at 3.6%, titanium oxide (Ti₂O) at 1.19%, and sodium oxide (Na₂O) at 1%. The mean values of chemical analysis results of shales in the Lower Anambra Basin, Nigeria showed that the predominantly chemical composition was silica (SiO₂) at 51.15%, and major constituents were alumina (Al₂O₃) at 15.75%, iron (III) oxide (Fe₂O₃) at 6.83%. Also, the shales were depleted in CaO at 2.35%, MgO at 1.44%, TiO₂ at 1.23%, K₂O at 0.86%, Na₂O at 0.14%, P₂O₅ at 0.11% and MnO at 0.06% (Okunlola *et al.*, 2023). The sample 1B closely resembled its constituents with Ifon shale from sedimentary basins in Nigeria, whereas showed that the predominantly composition was silica (SiO₂) at 63.30% and other major compositions were alumina (Al₂O₃) at 18.47%, potassium oxide (K₂O) at 2.36%, iron (III) oxide (Fe₂O₃) at 1.26% and titanium oxide (Ti₂O) at 1.02% (Okunlola *et al.*, 2023).

Sample 2A: The sample 2 A predominantly chemical constituent was calcium oxide (CaO) at 87.37%, and other constituents were silica (Si₂O) at 7.49%, alumina (Al₂O₃) at 2.44%, and iron (III) oxide (Fe₂O₃) at 1.17%. In the Anahita Temple of Kangavar in West Iran, the XRF analysis of three stone samples from the Temple (samples K3, K4, and K11) revealed that CaO is the primary component, ranging from 32% to 50% by weight, while SiO₂ varies between 2.83% and 11.60% by weight. The high CaO levels indicate the presence of limestone (Barnoo *et al.*, 2020). Therefore, sample 2A's higher CaO composition, at 87.37%, indicates that it was limestone.

Limestone Purity Classification: Sample 2A, 'limestone purity classification (CaCO₃ approximately 156%) was very high purity (CaCO₃% >98.5) according to the Harrison Classification, and limestone (CaCO₃% range between 100-95) according to the Teodorovich Classification, shown in (Table. 5) below (Surdashy and Aqrawi, 2023). Therefore, sample 2A was a limestone of very high purity.

Mineralogical characteristics: The natural stones were analyzed by X-ray diffraction method and the results are shown below (Table 6).

Table 5. Classification of limestone purity according to CaCO₃ ratio according to Harrison and Teodorovich (Surdashy and Aqrawi, 2023)

Harrison Classification		Teodorovich Classification	
Purity	CaCO ₃ %	Type of rock	CaCO ₃ %
Very High Purity	>98.5	Limestone	100-95
High Purity	97-98.5	Slightly dolomitic Limestone	95-80
Medium Purity	93.5-97	Medium dolomitic limestone	80-65
Low Purity	85-93.5	Highly dolomitic limestone	65-50
Impure	<85	Highly calcitic dolomite	50-35
		Medium calcitic dolomite	35-20
		Slightly calcitic dolomite	20-5
		Dolomite	5-0

Sample 1B: The predominantly stone mineral composition was quartz (SiO₂) at 30% and other major compositions were dickite (Al₂Si₂O₅(OH)₄) at 19%, Illite ((KH₃O)(AlMgFe)₂(SiAl)₄O₁₀(OH)₂) at 12%, sepiolite (Mg₄(Si₆O₁₅)(OH)₂) at 7.4%, calcite (CaCO₃) at 6% and nepheline ((NaK)AlSiO₄) at 5.4%. The mineralogical studies of shale conducted in the Lower Anambra Basin, Nigeria by x-ray diffraction showed that the primary composition was Kaolinite at 41.5%, besides major minerals were montmorillonite, chlorite, and illite; and non-clay minerals were quartz, ilmenite, and sillimanite (Okunlola *et al.*, 2023).

Sample 2A: The main stone mineral composition was calcite (CaCO₃) at 64.3% and other major constituents were quartz (SiO₂) at 8.7%, vaterite (CaCO₃) at 6.5%, and dolomite (Ca (MgCO₃)₂) at 5%. XRD analysis of the three samples (K3, K4, and K11) from the limestone of the Anahita Temple in Kangavar, West Iran, identified calcite (CaCO₃) as the predominant phase in the stone composition. Dolomite (CaMg(CO₃)₂) and quartz (SiO₂) were also detected alongside calcite in all the samples. Quartz is a minor phase in many sedimentary and carbonate stones (Barnoo *et al.*, 2020). The higher mineral constituents of calcite (CaCO₃) at 64.3% in sample 2A, indicated that it was a limestone. Limestone is a natural mineral primarily composed of calcium carbonate. Some calcium carbonate may have been partially replaced by magnesium carbonate, forming dolomite, which can constitute up to 46% by weight. Many limestones are exceptionally pure, containing less than 5% non-carbonate impurities (Oates, 1998).

Petrographic characteristics: The results for samples 1B and 2A were analyzed as follows;

General descriptions for sample 1B were;

Mineral Assemblage: The rock was grey to reddish brown and composed of 40-50% clay minerals and very fine round-to-sub round silt-sized quartz grains, opaque isotropic Iron oxide (hematite), and hydroxide (goethite) intergrown with quartz and weathered feldspar and clay matrix, few flakes of mica minerals mainly chlorite, biotite, and muscovite. calcite crystals and very few highly altered plagioclase feldspar grains (colorless, with grey interference colors).

Inclusions: The inclusions were mainly quartz subordinated with highly weathered perthitic K-feldspar and plagioclase feldspar fragments, very few chlorites, and biotite. Few grains of iron oxide and hydroxide, mostly goethite and hematite, and very few altered siderite crystals.

Descriptions: The rock was fine-grained, fissile (splits into thin pieces along the laminations), and laminated (made up of many thin layers) composed of very fine crystals of silt- and clay-sized crystals of clay minerals, angular to sub-angular grains of quartz and weathered plagioclase feldspars.

Table 6. Mineralogical compositions for samples 1B and 2A

S/N	Stone Composition		Sample Name: 1B		Sample Name: 2A	
	Name	Formula	Major Volume %	Minor Volume %	Major Volume %	Minor Volume %
1.	Quartz	SiO ₂	30		8.7	
2.	Dickite	Al ₂ Si ₂ O ₅ (OH) ₄	19			
3.	Illite	(KH ₃ O)(AlMgFe) ₂ (SiAl) ₄ O ₁₀ (OH) ₂	12			
4.	Chlorite	(MgFeAl) ₆ (SiAl) ₄ O ₁₀ (OH) ₈		2.4		
5.	Albite	NaAlSi ₃ O ₈		4.5		
6.	Nepheline	(NaK)AlSiO ₄	5.4			
7.	Hematite	Fe ₂ O ₃		3.6		
8.	Goethite	FeO (OH)		2.0		
9.	Calcite	CaCO ₃	6.0		64.3	
10.	Sepiolite	Mg ₄ (Si ₆ O ₁₅)(OH) ₂	7.4			
11.	Rutile	TiO ₂		1.0		
12.	Biotite	K(MgFe) ₃ (AlSi ₃ O ₁₀)(FOH) ₂		1.8		
13.	Kaolinite	Al ₂ Si ₂ O ₅ (OH) ₄		2.1		
14.	Vaterite	CaCO ₃			6.5	
15.	Siderite	FeCO ₃				4.8
16.	Dolomite	Ca(MgCO ₃) ₂			5.0	
17.	Diopside	CaMgSi ₂ O ₆				3.3
18.	Chloritoid	(FeMgMn) ₂ Al ₄ Si ₂ O ₁₀ (OH) ₄		2.8		
19.	Gibbsite	Al(OH) ₃				2.9
20.	Laumontite	Ca(AlSi ₂ O ₆) ₂				1.8
21.	Periclase	MgO				1.1
22.	Magnesite	MgCO ₃				0.6
23.	Muscovite	KAl ₂ (AlSi ₃ O ₁₀)(FOH) ₂				1.0
Total Percentages			79.8	20.2	84.5	15.5

particles, clastic and splintery texture, this makes this rock to easily splits into thin plates. The rock was formed where mud silts and clay-sized mineral crystals were deposited by slow transporting currents and became compacted at the bottom of water bodies. The presence of iron oxide and hydroxide in this rock such as hematite, goethite, and limonite which were observed to be isotropic in the microscope contributed to the reddish-brown color of this rock. The rock sample was characterized by having a highly weathered plagioclase feldspar grain (colorless, with grey interference colors). Quartz crystals in this sample were fine, round to sub round indicating transportation from a certain distance. The muscovite mica was the high-order-colored strands and strong pleochroic with basal to perfect cleavage, with the brown grains being biotite mica. Muscovite was colorless at Plane Polarized Light (PPL) and showed high birefringence at Cross Polarized Light (XPL) while Biotite was brown at PPL. The biotite and muscovite, flakes were randomly oriented. The grey and colorless grains were quartz and weathered feldspar. The possible name of the stone/rock was Shale. Shale simply splits into thin, mm-scale flakes along the sedimentary bedding, otherwise known as a shaley fissility. Furthermost shales indicate several kinds of grey, showing a high content of clay combined with small amounts of non-oxidized, ferrous iron-rich minerals. Brown or red shale might contain oxidized ferric iron minerals such as hematite (Fe₂O₃). Organic-rich shales were dark grey or black, whereas pale grey, and pale green (Merriman et al., 2003).

Sample 1B: Thin section micrographs description of sample 1B shown in (Figure.6) were;

- 1B(a): Colorless angular to sub-angular excellent quartz crystals Iron oxide mainly hematite fine crystals in the laminated shale.
 1B(b): Very fine brown biotite crystals with very high pleochroism. Iron oxide (hematite) melt shows a flowing texture surrounding and enclosed in the clay materials (grey with shades).
 1B(c): Yellowish brown weathered plagioclase and perthitic K-feldspar grains (colorless at PPL and with grey birefringence). Colorless quartz crystals and reddish-brown iron oxide.
 1B(d): Very fine calcite crystals (with high reflecting colors at the bottom of the micrography), Clay materials (black) oxide, colorless quartz crystals, weathered plagioclase feldspars, and iron oxide.

General descriptions for sample 2A were;

fragments of rock composed mainly of calcite, coarse to fine crystals of silt to sand-sized grains of quartz (some stained with iron oxide), altered feldspar (colorless, with grey interference colors), opaque iron oxide grains mainly hematite and magnetite intergrown with quartz and weathered feldspar, fossils, clay matrix. The rock is medium to coarse-grained composed of also few microcrystalline calcite matrixes (micrite), some few grains of quartz floating in a micritic groundmass, skeletons (fossils), altered siderite, and iron oxide stains.

Inclusions: Inclusions were mainly of calcite, iron oxide, clay materials, and round to sub-round fine to medium quartz subordinated with highly weathered perthitic K-feldspar and plagioclase feldspar with very few muscovite, and biotite.

Descriptions: The rock was clastic brown and composed of mainly calcite; gravel-sized (greater than 2.5 mm diameter) pebble-sized of 1.0cm to 3.5cm length. It had matrix-supported silt to sand-sized, rounded to sub-rounded gravel clasts cemented together, clay materials that fill the spaces between the clasts and cement them together. The pebbles in the rock were observed to be rounded and soft indicating they were transported far enough from their source and rubbed against each other. The rock was characterized by fine fracturing and cracking, veinlets of clay materials, carbonaceous grains, and sparry calcite crosscutting fine fractures in a micritic groundmass. Fossils observed in this rock are in parallel and randomly arrays filled with micrite, it appears to float in micritic groundmass. Most of the cavities were filled with recrystallized calcite, clay materials (black), and a few with iron oxide in a micritic groundmass. There were siderite crystals (grey) observed also in this rock. The clasts in this rock tend to feel smooth and rough when touched. The hardness and color of this rock is highly variable. due to the composition of various minerals with different colors and compositions.

Calcite in this rock contains euhedral crystals which form crystal clusters with perfect rhombohedral cleavage and effervescence in cold dilute HCl. Calcite had extremely high birefringence, resulting in pale, washed-out, and white interference colors. Polysynthetic twinning of calcite was observed also. This mineral shows high variable relief upon stage rotation. Flakes of mica minerals such as muscovite and biotite which have a very high pleochroism were observed. Muscovite was colorless at PPL and showed high birefringence at XPL while Biotite was brown at PPL. The possible name of the stone/rock was Limestone.

Sample 2A: Thin section micrographs description of sample 2A shown in (Figure.7) were;

2A(a): Siderite ($FeCO_3$) fragments (colorless at PPL), iron oxide stains in a micritic and sparry calcite groundmass. Cavities filled with recrystallized calcite and clay materials.

2A(c): Arrays of fossil prints in a micritic and sparry calcite groundmass, highly weathered plagioclase feldspar, quartz, voids filled by recrystallized calcite and clay materials.

2A(d): Micrite and sparry calcite filled by clay materials, clear quartz crystals were observed. Weathered plagioclase feldspar (yellowish brown) stained with iron oxide, fossils in sparry calcite, and micritic groundmass.

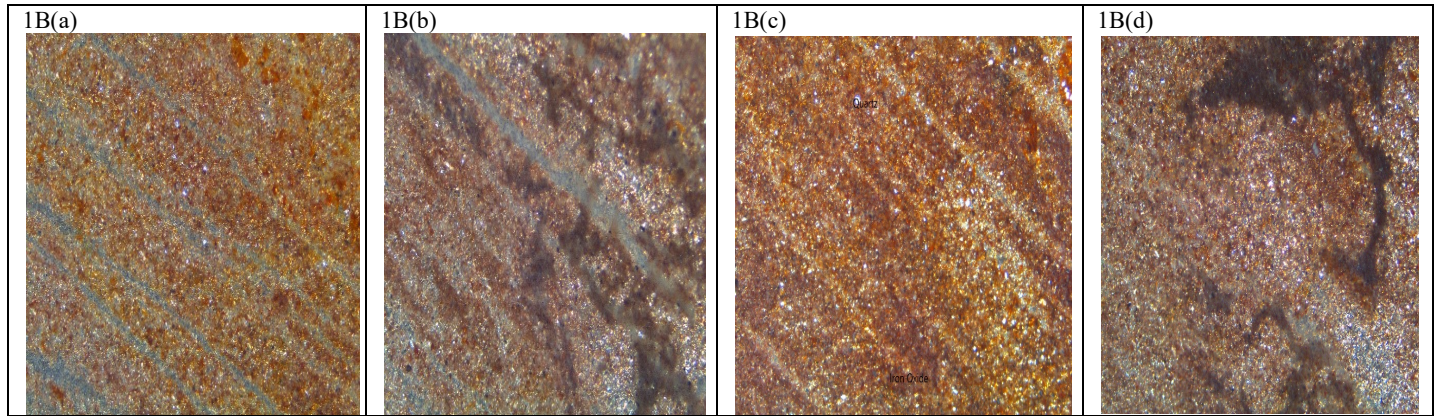


Figure 6. Thin section micrographs of sample 1B

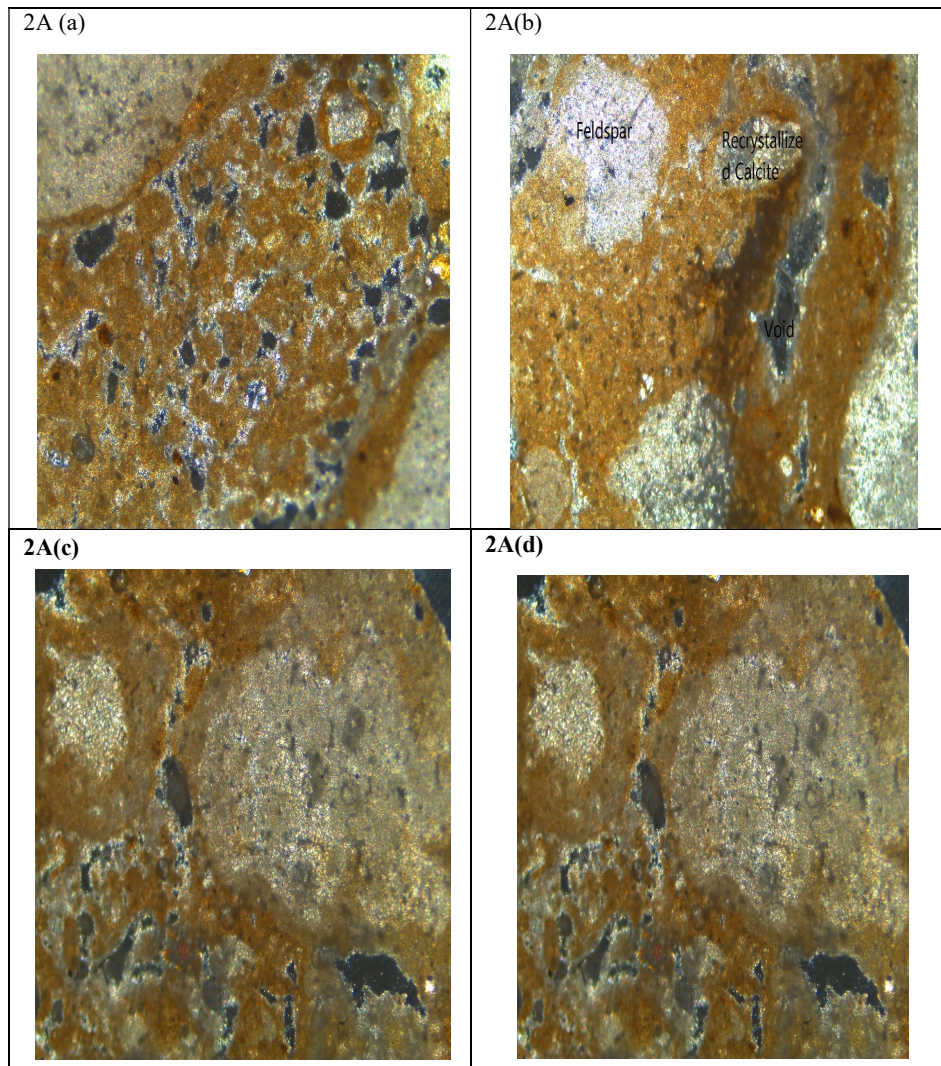


Figure 7. Thin section micrographs of sample 2A

2A(b): Highly weathered plagioclase feldspar stained with iron oxide, voids filled with clay materials, and fossils floating on clay groundmass. Biotite crystals (brown with strong pleochroism).

CONCLUSIONS AND RECOMMENDATIONS

Physical, chemical, mineralogical, and petrographic analysis revealed that; the two natural stone samples (1B and 2A) were shale and

limestone: shale, recommended as a building stone was composed of quartz, clay minerals, plagioclase feldspars, iron oxide, and hydroxide, calcite crystals, and mica-related minerals, and limestone, accepted as a building stone was poorly sorted with euhedral siderite grains (with high relief and dark Fe exsolution) and fragments, skeletons, and prints of fossils floating in a fine-grained micritic and sparry calcite groundmass, and characterized by iron oxide stains and occasional voids filled with calcite and clay material. Depositional structures observed include cavities filled with recrystallized calcite, fine fractures filled with iron oxide, iron oxide rims in fossil skeletons and siderite grains, strings of iron oxide cutting across the rocks, and voids filled with clay materials. Clay materials in the two natural stones samples were the result of prolonged extreme weathering of feldspars minerals (known as the mother of clay). Clay materials in these two samples were observed to contain tiny grains of rocks such as quartz and feldspars. When the clay is mixed with water it becomes soft gluey mud that can have various forms. Clay materials are plastic when wet, and coherent when dry. It is recommended that the conservation and restoration of the Fort Ikoma historical building in SENAPA, Tanzania, should involve using limestone for the foundation and floor-level walling and shale for the superstructure walling. The findings enhance awareness of historical materials and support the restoration of Fort Ikoma and similar buildings. I recommend limestone should be plastered to increase durability and reduce porosity.

REFERENCES

- Ali, B. S., Castro, J. J., Omi, S., and Nazimi, K. (2024). Exploration and Characterization of Dynamic Properties for Cultural Heritage Conservation: A Case Study for Historical Stone Masonry Buildings in Zanzibar. *Buildings*, 14(4). <https://doi.org/10.3390/buildings14040981>
- Ali, B., Khan, M. A., Hanif, M., Anwar, M., Ali, B., Yar, M., and Ahmed, I. (2023). Physico-mechanical and petrographic analysis of the Margalla Hill Limestone, Islamabad, Lesser Himalaya, Pakistan. *Carbonates and Evaporites*, 38(2). <https://doi.org/10.1007/s13146-023-00858-w>
- Amer, O., Abdel-Aty, Y., El-Hady, M. A., Aita, D., Torkey, A., and Hussein, Y. M. (2020). Multiscientific-based approach to diagnosis and characterization of historic stone-masonry walls: The mausoleum of al-imam al-shafi'i, Cairo (Egypt). *Mediterranean Archaeology and Archaeometry*, 20(2), 1–16. <https://doi.org/10.5281/zenodo.3746944>
- Amer, O., Aita, D., Mohamed, E. K., Torkey, A., and Shawky, A. (2021). Experimental investigations and microstructural characterization of construction materials of historic multi-leaf stone-masonry walls. *Heritage*, 4(3), 2390–2415. <https://doi.org/10.3390/heritage4030135>
- Barnos, V., Oudbashi, O., and Shekofteh, A. (2020). The deterioration process of limestone in the Anahita Temple of Kangavar (West Iran). *Heritage Science*, 8(1). <https://doi.org/10.1186/s40494-020-00411-1>
- Bukhari, S. A. A., Basharat, M., Janjuhah, H. T., Mughal, M. S., Goher, A., Kontakiotis, G., and Vasilatos, C. (2023). Petrography and Geochemistry of Gahirat Marble in Relation to Geotechnical Investigation: Implications for Dimension Stone, Chitral, Northwest Pakistan. *Applied Sciences (Switzerland)*, 13(3). <https://doi.org/10.3390/app13031755>
- Bureau of Indian Standards. (2003). *IS 1124 (1974): Method of test for determination of water absorption, apparent specific gravity, and porosity of natural building stones.*
- Cintra, D. C. B., Roehl, D. de M., Sánchez Filho, E. de S., Lourenço, P. B., and Mendes, N. (2024). Methodologies for assessing the structural integrity of historic masonry domes and vaults. *Revista IBRACON de Estruturas e Materiais*, 17(4). <https://doi.org/10.1590/s1983-41952024000400006>
- CML. (2000). *Laboratory Testing Manual.*
- Degryse, P., Elsen, J., and Waelkens, M. (2002). *Study of ancient mortars from Sagalassos (Turkey) in view of their conservation.*
- Hagan, P. (2009). *A Study on the Effect of Moisture Content on Rock Cutting Performance.* <https://www.researchgate.net/publication/30384641>
- Hernández, A. C., Sanjurjo-Sánchez, J., Alves, C., and Figueiredo, C. A. M. (2024). Provenance Studies of Natural Stones Used in Historical Buildings of the Peninsula de Barbanza, Galicia, Spain (North-Western Iberia). *Minerals*, 14(6), 595. <https://doi.org/10.3390/min14060595>
- Lourenço, P. B. (2002). Computations on historic masonry structures. *Progress in Structural Engineering and Materials*, 4(3), 301–319. <https://doi.org/10.1002/pse.120>
- Lucian, C. (2008). Engineering Properties of Building Materials in Historic Buildings in Bagamoyo (Tanzania). In *Certified International Journal of Engineering and Innovative Technology (IJEIT)* (Vol. 9001, Issue 9).
- Merriman, R. J., Highley, D. E., and Cameron, D. G. (2003). *Definition and characteristics of very-fine-grained sedimentary rocks: clay, mudstone, shale, and slate.* www.thebgs.co.uk
- Mifkovic, Michael M., and Dot. (2012). *DEFINITIONS OF TERMS RELATING TO SPECIFIC GRAVITY.* http://www.dot.ca.gov/hq/esc/ctms/pdf/lab_safety_manual.pdf
- Mustafaraj, E. (2013). *Structural assessment of historical buildings: a case study of five Ottoman Mosques in Albania.*
- Oates, J. A. H. (1998). *Lime and Limestone.*
- Okunlola, O., Lydia, A. U., Umaru, A. O., Kazapoe, R. W., and Olisa, O. G. (2023). Mineralogy and Geochemistry of Shale Deposits in the Lower Anambra Basin, Nigeria: Implication for Provenance, Tectonic Setting and Depositional Environment. *Economic and Environmental Geology*, 56(6), 799–816. <https://doi.org/10.9719/EEG.2023.56.6.799>
- Pappalardo, G., Mineo, S., Caliò, D., and Bognandi, A. (2022). Evaluation of Natural Stone Weathering in Heritage Building by Infrared Thermography. *Heritage*, 5(3), 2594–2614. <https://doi.org/10.3390/heritage5030135>
- Patil, S. M., Kasthurba, A. K., and Patil, M. V. (2021). Characterization and assessment of stone deterioration on Heritage Buildings. *Case Studies in Construction Materials*, 15. <https://doi.org/10.1016/j.cscm.2021.e00696>
- Pereira, D. (2023). The Value of Natural Stones to Gain in the Cultural and Geological Diversity of Our Global Heritage. In *Heritage* (Vol. 6, Issue 6, pp. 4542–4556). MDPI. <https://doi.org/10.3390/heritage6060241>
- Pereira, D. (2024). Stones that Tell Stories. *Geoheritage*, 16(2). <https://doi.org/10.1007/s12371-024-00944-y>
- Pereira, D., and Marker, B. (2016). The value of original natural stone in the context of architectural heritage. *Geosciences (Switzerland)*, 6(1). <https://doi.org/10.3390/geosciences6010013>
- Surdashy, A. A., and Aqrabi, A. M. (2023). Evaluation of Cretaceous-Tertiary Limestone for Building and Dimension Stones in Erbil, Kurdistan Region of Iraq. *Iraqi Geological Journal*, 56(2), 48–68. <https://doi.org/10.46717/igj.56.2E.4ms-2023-11-9>
